Circular RNAs correlate with DNA damage in ageing human placental tissue and in stillbirth

Keywords: stillbirth, placenta, pregnancy, ageing, DNA, circular RNA, double stranded breaks

Anya L. Arthurs[1,2*], Matilda R. Jackson[3,4,5], Dylan McCullough[1,2], Hamish S. Scott[3,4,6,7,8], Christopher P. Barnett[6,9], Stuart T. Webb[1,2,3], Melanie D. Smith[1,2], Tanja Jankovic-Karasoulos[1,2], Gustaaf A. Dekker[10], Claire T. Roberts[1,2].

[1] Flinders Health and Medical Research Institute, Flinders University, Adelaide, South Australia, Australia 5042

[2] College of Medicine and Public Health, Flinders University, Adelaide, South Australia, Australia 5042

[3] Department of Genetics and Molecular Pathology, SA Pathology, Adelaide, South Australia, Australia 5000

[4] Centre for Cancer Biology, an alliance between SA Pathology and University of South Australia, Adelaide, South Australia, Australia 5000

[5] Australian Genomics, Parkville, Victoria, Australia

[6] Adelaide Medical School, The University of Adelaide, Adelaide, South Australia, Australia

[7]ACRF Genomics Facility, Centre for Cancer Biology, an alliance between SA Pathology and University of South Australia, Adelaide, South Australia, Australia

[8] UniSA Clinical and Health Sciences, University of South Australia, Adelaide, South Australia, Australia

[9] Paediatric and Reproductive Genetics Unit, South Australian Clinical Genetics Service, Women's and Children's Hospital, North Adelaide, South Australia, Australia

[10] Department Obstetrics and Gynecology, Lyell McEwin Hospital, The University of Adelaide, Adelaide, South Australia.

* Corresponding author: anya.arthurs@flinders.edu.au

31 # Graphical Abstract

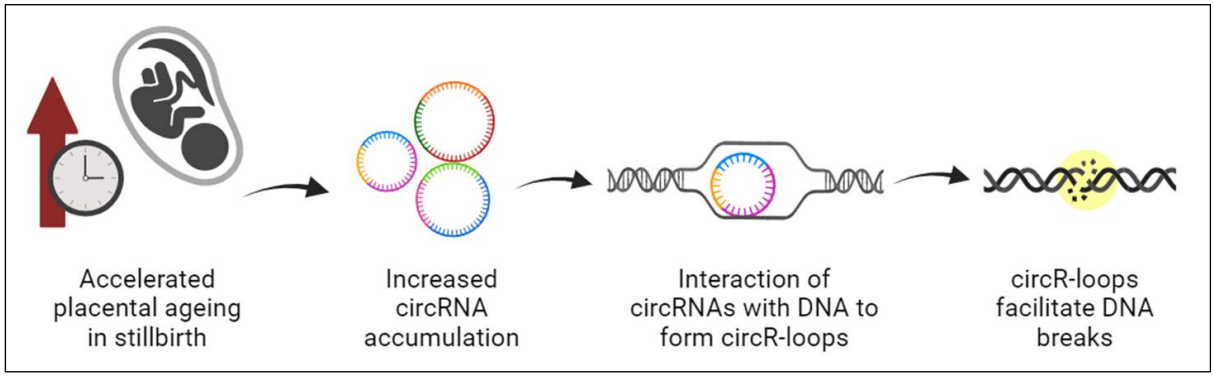

32

33

34 # Abstract

35 Unexplained stillbirth is hypothesised to occur due to premature placental ageing, with
36 unexpected deterioration of placental function for gestational age. Circular RNAs (circRNAs)
37 are enzyme resistant RNA molecules that accumulate in ageing tissues. Furthermore, circRNAs
38 bind gDNA directly, forming circRNA:DNA complexes which can induce DNA breaks. This
39 study investigated circRNA accumulation with gestational age in healthy and stillbirth
40 placentae and determined whether circRNAs directly interact with placental DNA causing
41 DNA damage.

42 Placenta samples (n=60 term uncomplicated; n=4 unexplained stillbirth, 23, 26, 31, 34 weeks'
43 gestation) were assessed for DNA damage using an alkaline Comet Assay. Expression levels
44 of 6 candidate circRNAs (circ_0009000, circ_0024157, circ_0061017, circ_0036877,
45 circ_0054624 and circ_0111277), and their linear transcripts, were quantified using qPCR.
46 Physical interaction of candidate circRNAs with DNA was confirmed by DNA:RNA
47 ImmunoPrecipitation (DRIP). The effect of circ_0009000 knockdown in HEK293T cells was
48 assessed following transfection with either a siRNA (designed to knockdown circ_0009000)
49 or a scrambled siRNA control, at 5, 10 and 20 nM final concentrations using Lipofectamine
50 RNAiMax. DNA damage was assessed by Comet Assay. Compared with earlier gestations (37,
51 38, 39 and 40 weeks'), placental DNA damage and expression of all 6 candidate circRNAs,

52 but not their linear transcripts, were increased in 40 and 41+ weeks' gestation samples, and in
53 stillbirth.
54 DRIP-qPCR signal size was significantly larger in term placentae than in enzyme-treated
55 controls, confirming that all candidate circRNA loci bind to placental DNA.
56 Depletion of circ_0009000 by specific siRNA in HEK293T cells, significantly reduced DNA
57 damage compared to control.
58 Stillbirth placentae show accelerated ageing with premature accumulation of candidate
59 circRNAs (first evidence in humans) at levels consistent with older gestation tissue.
60 Importantly, these circRNAs bind to DNA and circ_0009000 causes DNA breaks in placenta.
61 Therefore, circRNAs (circ_0009000, circ_0024157, circ_0061017, circ_0036877,
62 circ_0054624 and circ_0111277) play a role in placental ageing and associate with stillbirth,
63 likely via DNA damage.
64

65 # 1. Introduction

66 Stillbirth is defined as a fetal death prior to birth of a baby of either (i) ≥20 completed weeks'
67 of gestation or, (ii) ≥400g birthweight[1]. Annually there are 2 million stillbirths worldwide[2],
68 with ~2300 occurring every year in Australia, at a rate unchanged for decades[1]. Whilst some
69 cases of stillbirth can be attributed to fetal congenital abnormalities, many cases of stillbirth
70 are "unexplained", where autopsy that includes fetal genetics does not establish cause.
71 Although some risk factors have been identified[1,3], the aetiology of unexplained stillbirth is
72 unknown, and is thus impossible to prevent. One theory for the mechanism underpinning
73 unexplained stillbirth is premature placental ageing.
74
75 The placenta is a transient organ with a finite life in gestation. Placental ageing is a normal
76 phenomenon resulting in physical changes in late gestation without fetal compromise.
77 Accelerated placental ageing can occur in stillbirth, leading to reduced placental functional
78 capacity for fetal support. Whilst markers of tissue ageing, including measures of DNA
79 damage[3-5], are reportedly irregularly high in stillbirth placentae, a direct measure of DNA
80 breaks has not previously been reported.
81
82 Tissue ageing has been associated with circular RNAs (circRNAs). circRNAs can be generated
83 from most genes and encompass one or multiple exonic or intronic regions of RNA.
84 Importantly, they display tissue-specific patterns of expression, making them unique to their
85 tissue of origin as well as the genome of the individual. circRNAs are inherently stable, hence
86 they can accumulate in tissues with age (previously shown in *Drosophila melanogaster,*
87 *Caenorhabditis elegans* and murine models[6-8]).
88
89 Whilst circRNAs have many functions[9], of importance is their ability to directly bind to

90 genomic DNA, forming a circRNA:DNA complex (termed a 'circR-loop')[10]. Due to the steric
91 hinderance, the presence of a circR-loop can cause RNA polymerase II to stall during
92 transcription, subsequently leading to a DNA break. This often results in genomic instability[11],
93 cellular senescence or apoptosis[12], and cell death[13].
94
95 Given that unexplained stillbirth may be due to premature placental ageing, and that circRNAs
96 accumulate in ageing animal tissues, we sought to determine whether circRNAs accumulated
97 with gestational age in healthy and stillbirth placentae. We accomplished this by quantifying
98 RNA (both circRNA-enriched and total) to ensure no significant changes in transcript numbers
99 with gestational age. We also quantified circRNA abundance along with all cognate linear
100 transcripts for each circRNA, to ensure changes in circRNA abundances were due to
101 accumulation, not simply products of alternative splicing. We further investigated whether
102 select circRNAs bind to DNA to form circR-loops and induce DNA breaks. This study provides
103 novel evidence of circRNA accumulation in ageing human tissue and proposes a potential
104 mechanism for stillbirth pathogenesis.

105 # 2. Methods

106 ## 2.01 Tissue Samples

107 *Healthy placentae from 37-41+ weeks' gestation:* Term placentae were obtained at the Lyell
108 McEwin Hospital in Elizabeth, South Australia, from women recruited as part of the Screening
109 Tests to predict poor Outcomes of Pregnancy (STOP) (2015–2018) cohort study[14]. The study
110 was registered with the Australian and New Zealand Clinical Trials Registry (ACTRN
111 12614000985684). All placentae were associated with uncomplicated pregnancies and were
112 collected from white women. Tissue biopsies from placentae were washed in phosphate-
113 buffered saline (PBS) before being snap frozen and held in liquid nitrogen for 15 min, then
114 stored at -80°C. Ethics approval was obtained from the Women's and Children's Health
115 Network Human Research Ethics Committee (HREC/14/WCHN/90; STOP). All women
116 provided written informed consent.

117

118 *Placentae collected from unexplained stillbirths:* Small placental biopsies from unexplained
119 stillbirth cases were obtained from women who had been recruited in to the NHMRC- and
120 GHFM-MRFF-funded Genomic Autopsy Study[15]. Placental biopsies were obtained as part of
121 the standard autopsy procedure and were stored at -80°C as approved by the Human Ethics
122 Committee of the Women's and Children's Health Network, South Australia, Australia
123 (HREC/15/WCHN/35) and Melbourne Health as part of the Australian Genomics Health
124 Alliance protocol (HREC/16/MH/251). Informed consent was obtained to allow access to
125 relevant medical information and subsequent storage of anonymized samples, genomic data
126 and/or medical information in relevant databases and publications.

127

128 **2.02 RNA Extraction**

129 Healthy term and stillbirth placental tissues (25mg) were weighed and washed with phosphate-
130 buffered saline (PBS). Tissue was disrupted by homogenizing for 3.5 min at 30 Hz
131 (TissueLyser, QIAGEN) in 1mL *TRIzol Reagent* (Sigma-Aldrich). The manufacturer's
132 protocol was then followed to isolate total RNA. The purity and integrity of extracted RNA
133 samples were determined using the Experion™ (BioRad) and samples used had an RNA
134 Quality Index ≥ 8. Samples were split into two aliquots, with one aliquot to be assessed for
135 circRNA expression levels and the other to be assessed for linear transcript expression levels.
136 Samples to be assessed for circRNA expression levels were heated to 70°C for 5 mins, then
137 immediately cooled below 40°C before incubation with RNase R (10U / reaction; Astral
138 Scientific) for 1 h at 40°C. This step was essential to digest all linear RNAs, leaving only lariat
139 or circular RNA structures.

140 **2.03 RNA Quantification**

141 Total RNA for each sample, after incubation of 1 µg of RNA either with RNase R or untreated,
142 was quantified using the Qubit 2.0 fluorimeter (Thermo Fisher Scientific). As per Drula, *et*
143 *al.*[16], Qubit measurement was accomplished with the Qubit™ RNA High Sensitivity (HS)
144 assay kit using 1 µL of the RNA sample, 198 µL of the kit Qubit working solution and 1 µL of
145 the provided fluorophore, as per manufacturer's instructions. RNA amount was normalised
146 based on the standard curve and input and compared between RNase R treated and untreated
147 groups per sample to quantify bulk circRNA abundance.

148 **2.04 cDNA Synthesis and Quantitative Polymerase Chain Reaction (qPCR)**

149 Synthesis of complementary DNA (cDNA) was conducted beginning with 1μg of total RNA
150 using the QuantiNova Reverse Transcription Kit (QIAGEN) according to the manufacturer's
151 protocol. qPCR was performed in triplicate and conducted with SYBR Green (QIAGEN)
152 according to manufacturer's instructions, with *YWHAZ, GAPDH* and *ACTB* as housekeeping
153 genes (all primer sequences in **Table 1**). Custom divergent primers were designed for each
154 circRNA, flanking the backsplice junction, with an amplicon size <300 base pairs. As an
155 additional confirmation of amplification specificity, all primers were assessed using the Primer
156 design BLAST tool[16]. Furthermore, primer specificity was confirmed via melt curve analysis
157 from qRT-PCR. The qPCR conditions were PCR initial activation at 95°C for 5 min followed
158 by 50 cycles of 95°C for 15s, T_m (detailed in **Table 1**) for 20s and 72°C for 20s. qPCR results
159 were analysed using the 2-ΔΔCT method[17]. Samples were sorted into groups depending on
160 gestational age of tissue (see **Table 2** for numbers and characteristics of women's samples
161 used).
162

163 **2.05 Cell culture and siRNA transfection**

164 HEK293T cells (CRL-3216; ATCC) were cultured (n = 3, in triplicate; final n = 9) at 37°C in
165 5% CO_2 using Dulbecco's Modified Eagle Medium with GlutaMAX supplement (Gibco) and
166 10% v/v fetal bovine serum (Sigma-Aldrich). siRNA was produced by Thermo Fisher
167 Scientific (Silencer Select siRNA). siRNA sequence was designed to be complementary to the
168 backsplice junction of circ_0009000 (sequence:
169 CTGCTCCACGGCTTGGCCACCTGTTCCCA; scrambled siRNA sequence:
170 GACCTCGTGCTCGTCACCTCCGACTCGTC). Cells were transfected (24-well plates) with
171 the siRNA and scrambled siRNA at 5, 10 and 20 nM final concentrations using Lipofectamine
172 RNAiMAX (Life Technologies) following the manufacturer's instructions. After optimisation,

173 experiments proceeded with 10 nM final concentration (as the lowest siRNA concentration
174 producing the desired level of knockdown). At 96 hours post-siRNA transfection cells were
175 collected and either (i) immediately used for Comet assay or (ii) snap frozen in liquid nitrogen
176 prior to storage at −80°C for subsequent RNA analysis.
177

178 **2.06 Comet Assay**

179 The Abcam Comet Assay Kit (ab238544; Abcam) was used to assess DNA damage in isolated
180 trophoblasts. Approximately 25mg tissue (stored at -80°C) in 1.5mL ice-cold PBS containing
181 20 mM EDTA (without Mg^{2+} and Ca^{2+}) was minced using dissection scissors. The tissue
182 suspension settled for 5 min (4°C) prior to removal of the supernatant for centrifugation (700xg,
183 2 min). The supernatant was then discarded, and the cell pellet was resuspended at $1x10^5$
184 cells/mL in ice-cold PBS (without Mg^{2+} and Ca^{2+}). Cell samples were combined with Comet
185 Agarose at a 1/10 (v/v) ratio, mixed by pipetting and transferred onto pre-prepared Comet
186 Agarose glass slides. Slides were incubated (in the dark, 15 min, 4°C) prior to immersion in
187 Lysis Buffer (14.6g NaCl, 20 mL EDTA [provided], 10 mL 10X Lysis Solution [provided], 10
188 mL DMSO, volume adjusted to 90 mL with deionised H_2O, pH = 10.0) for 45 min (in the dark,
189 4°C). Slides were then transferred and immersed in Alkaline Solution (1.2g NaOH, 0.2 mL
190 EDTA [provided], volume adjusted to 100 mL with deionised H_2O) for 30 min (in the dark,
191 4°C).
192

193 Alkaline electrophoresis was then performed as follows: slides were carefully transferred from
194 the Alkaline Solution into the electrophoresis chamber containing Alkaline Electrophoresis
195 Solution (1L of 300 mM NaOH, 1 mM EDTA; pH > 13, 4°C) and electrophoresis conditions
196 applied (30V, 300mA, 30 min). Following electrophoresis, slides were carefully washed by

197 immersion in deionised H_2O (3 washes at 2 min each; 4°C) prior to submersion in 70% EtOH
198 (5 min, 4°C), then dried at room temperature. Slides were visualised by staining with the
199 supplied Vista Green DNA Dye and imaged by epifluorescence microscopy using a FITC filter.
200
201 The DNA integrity of 100 cells per placenta was analysed using CometScore 2.0 software
202 (RexHoover.com). The fluorescence intensity of the comet 'tail' was used as a measure of
203 DNA damage (indicated as tail DNA%). Tail DNA was shown as a percentage increase in
204 damage relative to averaged control samples.
205

206 **2.07 DNA:RNA ImmunoPrecipitation (DRIP)**

207 DRIP was performed according to steps 3-25 in the protocol published by Sanz, *et al.* 2019[18],
208 with some notable exceptions. As tissue was used as a starting material instead of cultured
209 cells, tissue was first prepared as follows before progressing to step 3 of the protocol.
210
211 About 50mg frozen placental villous tissue was submerged in 1mL RLT+ buffer (QIAGEN)
212 with added 0.01% (v/v) β-mercaptoethanol and 0.5% (v/v) Reagent DX (QIAGEN) with 1g
213 beads. Tissue was disrupted by homogenizing for 3.5 min at 30 Hz (TissueLyser, QIAGEN).
214 Cell suspensions were centrifuged (3 min, max speed, 4°C) prior to removal of the supernatant.
215 The cell pellet was washed (sterile DPBS, 5mL) before centrifugation (3 min, 1000 RPM, 4°C)
216 and removal of the supernatant. Steps 3-25 of the protocol[18] were then followed.
217

218 **2.08 Statistical Analysis**

Statistical analysis for differences between groups for qPCR and Comet Assay data was undertaken using SPSS Statistics Software. Outliers were removed from the data using a Grubbs' test. Data were assessed for normality distribution and either a Kruskal-Wallis test or two-way ANOVA tests conducted. Adjustments were made for multiple comparisons (Tukey's). Differences between groups were considered significant at $p < 0.05$.

Table 1. *Primer sequences and melt temperatures (T_m) used for qPCR*

Gene	Transcript	Forward primer	Reverse primer	T_m
CRHR2	XM_024446665.1	ATGGACGCGGCACTGCT	ACTGCAGCCTGGCGCT	57
	XM_017011752.2	TCCTACTGCAACACGACCTT	GTTGATCTTTGAGGCCCACG	59
	NM_001202483.2	AGAAAGAGATGTGTGCCAAGC	CCAGAGGAAGAAGGTGGAGG	58
	NM_001202482.2	CTCACTCTCGCGTCCACTC	GTTGATCTTTGAGGCCCACG	59
	NM_001202481.1	GGTCAAATGGGAAGAGAGCC	GTGTTGTACTTGACGCCGTT	58
	NM_001202475.1	CATGACCCTCACCAACCTCT	AAGGTCGTGTTGCAGTAGGA	58
	Circular: circ_0009000	TGGCTACAATTCCTGCTCCA	ACATCTGCTGCTTTGTGTGG	59
CWF19L2	XM_017017239.2	AGATGGTGGATTAAGCTGGCT	GAATGGACTCACGCTCTGGA	59
	XR_947795.2	CCAGAAAGGGAGTATGAACAAAC	CCATGTCACCCACTTCCTTG	57
	NM_152434.3	AGCCATCGGAAACCAGTACT	CCATGTCACCCACTTCCTTG	58
	XM_011542620.3	TCATGGAGTCGCTCTGATGG	ACATCAGGGAATGGGCTCTT	58
	Circular: circ_0024157	AGAAGTGATATACCATTCTTAAATGTA	GATAAATTACAAAATTACATGGATAA	53
RAB22A	NM_020673.3	TATTGTGTGGCGGTTTGTGG	TCTTGTCCAGCTGTATCCCA	58
	Circular: circ_0061017	CCCATTGGCTGAACTCTTCC	AGCCACTACACTTGTTCTTGA	57
FURIN	NM_001382622.1	GCATCATCGACATCCTCACC	GTCTCCACGTCATTCTCGGT	58
	NM_002569.4	ACATCCTCACCGAGCCCA	GACTCTCGGCTGCTCTGG	59
	NM_001382619.1	GTGCAGTCCTCCCTCGAC	TCACTCCTCGATGCCAGAAG	59
	NM_001289823.2	CGGTCGCCTGGAAAAGTT (distinguished by product size)	CTGGACGATGGCATCGAGA	58
	NR_168464.1			
	NM_001382620.1	GACTCGGGTGCGGGATC	TGTTGCTGCTACCACCCATA	58
	NM_001382621.1	CCAAGAACACAGCCAGGAAG	TACCACCCATAGCAACCAGG	58
	NM_001289824.2	GGTTTGAGACAAACTGGGACTAG	GACCAAGGTTCCTGTTGCTG	58
	Circular: circ_0036877	TTTGTAAGATGCTGGGTTGGTG	ACTGCATCTGTCACCTCGC	57

Gene	Transcript	Forward primer	Reverse primer	T_m
PNPT1	NM_033109.5	CCTTCCCAGTTTATGCCTTTGG	AAAGAGCGGTCTAATTGAACGAT	60
	Circular: circ_0054624	AGCATGTTAGGCAATGTTGAT	TTTACTGACCGCTGTGACCA	60
PAPPA2	XM_005245422.3	GCATCTCAGCTGTGGCTCTA	AGTTACTGGGAGCCGAAAGAC	56
	Circular: circ_0111277	AGTCGATGGATTCCTCTCAT	AAGTTGTTCATCACTCTGTT	55
YWHAZ		ACCGTTACTTGGCTGAGGTTGC	CCCAGTCTGATAGGATGTGTTGG	60
GAPDH		TCAAGGCTGAGAACGGGAAG	CGCCCCACTTGATTTTGGAG	60
ACTINB		CACCATTGGCAATGAGCGGTTC	AGGTCTTTGCGGATGTCCACGT	60

3. Results

3.01 Cohort Characteristics

Placenta samples were available from n = 60 women who had healthy pregnancies (n = 12 per gestational group) and n = 4 women who experienced stillbirth. All stillbirths had been assessed by clinical pathologists as "unexplained fetal deaths", with no noted congenital anomalies. Maternal and birth characteristics are presented in **Table 2**.

Table 2. *Characteristics of women and infants from the study by gestational age group (weeks')*

	Gestational Age group (weeks')					**Stillbirth**
	37	**38**	**39**	**40**	**41+** †	
Maternal age (years)	28.7 ± 1.5	24.1 ± 2.9	25.9 ± 1.9	28.3 ± 4.5	26.8 ± 4.2	#1: 35 #2: 26 #3: 33 #4: 28
Maternal BMI (kg/m^2)	26.4 ± 5.8	27.2 ± 9.1	23.1 ± 4.3	20.8 ± 4.1	23.4 ± 6.2	#1: DM #2: DM #3: DM #4: 22.8
Smoking status*	1/12	2/12	1/12	3/12	2/12	#1: DM #2: DM #3: DM #4: N
Gestational age (weeks)	37.1 ± 0.9	38.0 ± 0.3	39.1 ± 0.7	40.0 ± 0.4	41.5 ± 0.3	#1: 23 #2: 26 #3: 34 #4: 31
Birthweight (g)	2962 ± 325	3345 ± 465	3089 ± 201	3702 ± 161	3513 ± 277	#1: 256 #2: 800 #3: 2546 #4: 1140
Fetal sexˆ	XX = 6 XY = 6	XX = 6 XY = 6	XX = 7 XY = 5	XX = 6 XY = 6	XX = 6 XY = 6	#1: XX #2: XY #3: XY #4: XX

Data are presented as mean ± standard error of the mean.
DM = Data Missing, as data were not available at the time of sample collection.
* Smoking status as self-reported by patient at time of delivery. X/12 indicates the number of women who reported YES to smoking while pregnant out of the total 12 women. For stillbirths, Y = Yes, N = No.
ˆ Where XX = female, XY = male.
† The group "41+ weeks' gestation" is defined as delivery at 41+0 through to 41+6 weeks' gestation.

15 **3.02 DNA damage is increased in placentae from 40 and 41+ weeks' gestation,**

16 **and in stillbirth**

17 DNA damage was assessed using the Comet Assay that yields a Tail DNA% metric, an
18 indication of the level of DNA damage in placental cells. Representative images of healthy
19 cells (**Figure 1A**) and DNA damaged cells (**Figure 1B**) are included for reference. Tail DNA
20 % was significantly higher in cells from placentae sampled at 40 weeks' gestation compared
21 with 37 and 38 weeks' ($p_{37} = 0.0381$, $p_{38} = 0.0203$; **Figure 1C**). Tail DNA% was significantly
22 higher in cells from placentae sampled at 41+ weeks' gestation compared with 37, 38, 39 and
23 40 weeks' (all $p < 0.0001$) as well as in placentae from stillbirths compared with 37, 38, 39 and
24 40 weeks' gestation ($p_{37} < 0.0001$, $p_{38} < 0.0001$, $p_{39} < 0.0001$, $p_{40} = 0.0001$).

25

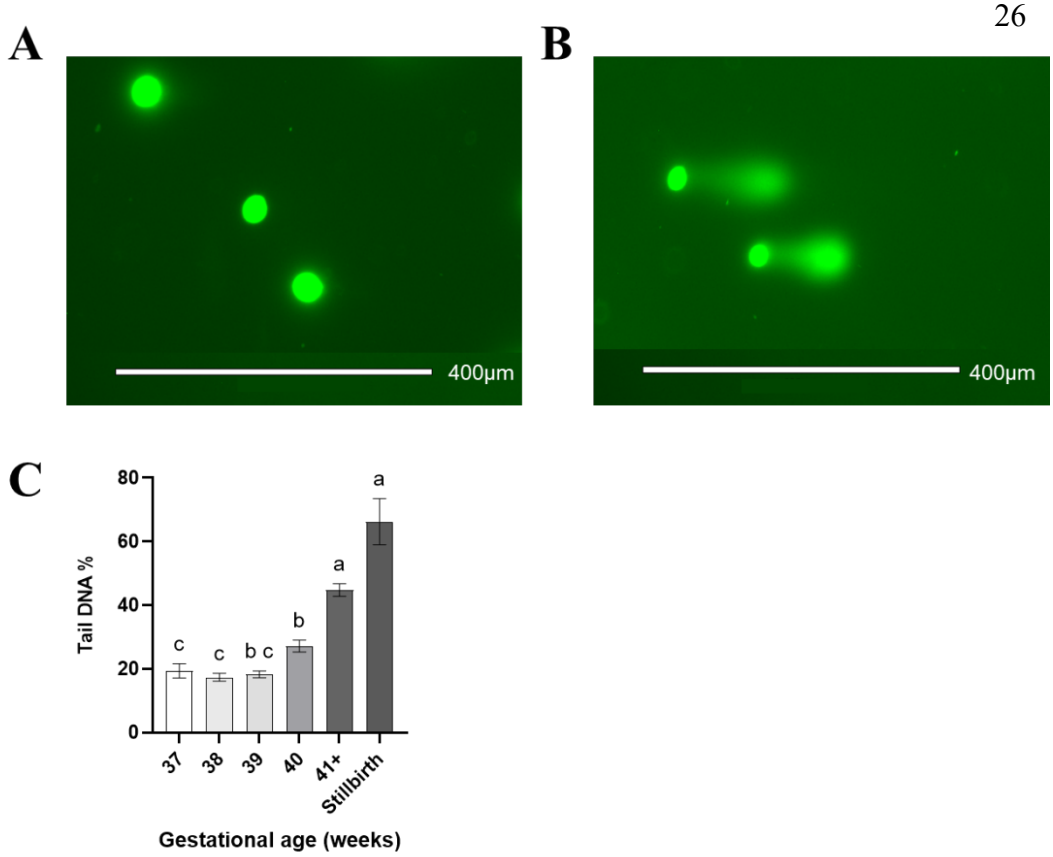

Figure 1. *Representative images of* ***(A)*** *healthy cells and* ***(B)*** *DNA damaged cells, as imaged using epifluorescent microscopy after performing a Comet Assay.* ***(C)*** *Levels of DNA damage, as assessed by Tail DNA %, in isolated cells from 37, 38, 39, 40 and 41+ uncomplicated, and stillbirth, placentae. n = 12 placentae / uncomplicated gestational group, n = 4 stillbirth placentae. 100 cells analysed following Comet Assay, per placenta. Data are presented as mean ± standard error of the mean. Different letters represent statistically significant (p < 0.05) differences.*

28 **3.03 Abundance of total RNA, and circRNA, is unchanged with gestation and**
29 **in stillbirth**

30 RNA concentration was measured in placenta samples from 37, 38, 39, 40 and 41+ weeks'
31 gestation, and in placenta samples from stillbirths. RNA was extracted from each sample, then
32 split into two aliquots; the first was untreated (total RNA) while the second was digested with
33 RNase R (leaving only circRNAs). RNA concentration and abundance of total RNA and RNase
34 R-digested RNA were assessed to determine whether these changed across gestation or in
35 stillbirth.
36 Both RNA concentration (**Figure 2A-B**) and relative abundance level (**Figure 2C**) total RNA
37 and RNase R-digested RNA was unchanged with gestation and in stillbirth.

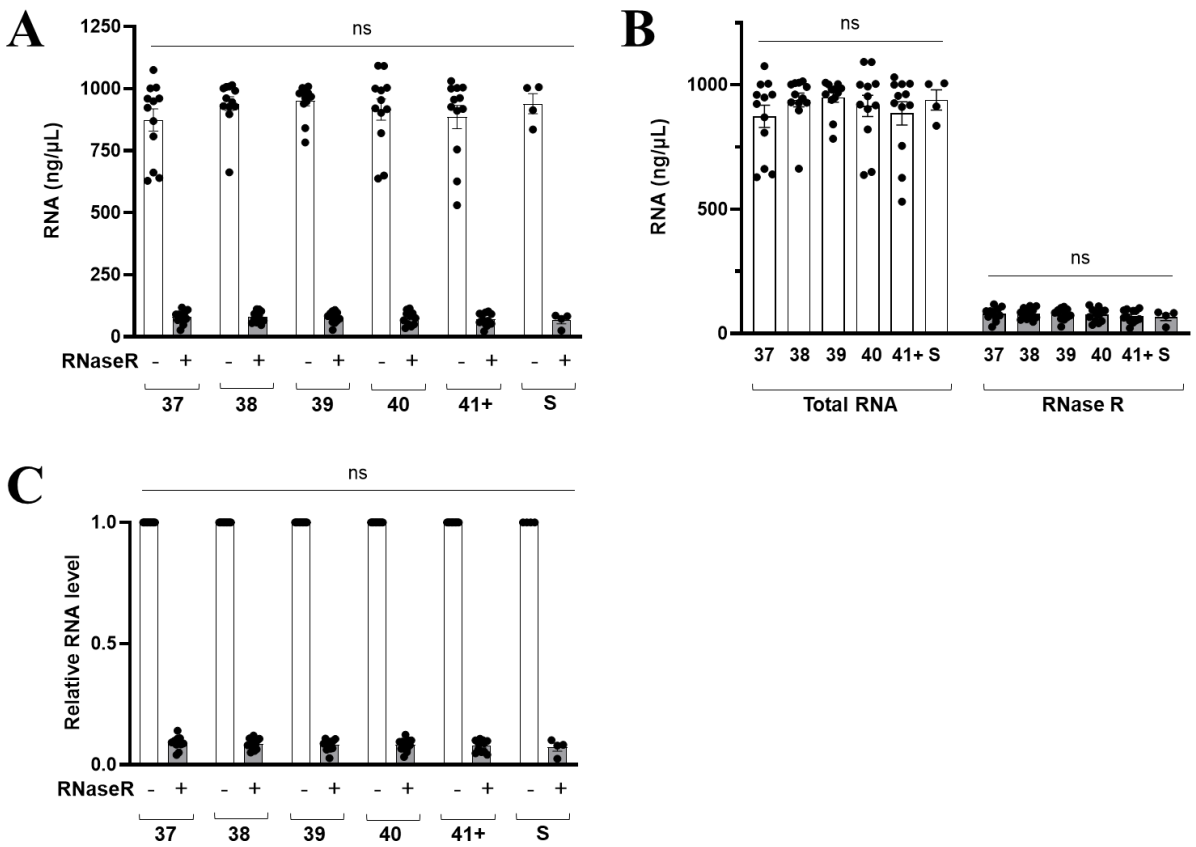

Figure 2. (A-B) *RNA concentration (ng / µL) and* ***(C)*** *abundance (as fold change of RNase R-depleted RNA relative to total RNA) in isolated cells from 37, 38, 39, 40 and 41+ uncomplicated, and stillbirth (S), placentae. n = 12 placentae / uncomplicated gestational group, n = 4 stillbirth placentae. Data are presented as scatter plots with bars and indicate mean ± standard error of the mean. ns = not significant.*

39 **3.04 Abundance of circ_0009000, but not linear *CRHR2* mRNA gene variants,**

40 **is increased in placentae from 40 and 41+ weeks' gestation, and in stillbirth**

41 Relative abundance of circ_0009000, expressed as fold change compared to abundance in
42 placentae at 37 weeks' gestation, was significantly increased in cells from placentae sampled
43 at 40 weeks' gestation compared with 37 and 38 weeks' ($p_{37} = 0.0005$, $p_{38} = 0.0079$; **Figure**
44 **3A**). circ_0009000 abundance was also significantly increased in cells from placentae taken at
45 41+ weeks' gestation compared with 37 and 38 weeks' (all $p < 0.0001$), as well as in placentae
46 from stillbirths compared with 37 and 38 weeks' gestation ($p_{37} < 0.0001$, $p_{38} = 0.0006$).
47
48 Abundance of linear *CRHR2* mRNA (relative to *YWHAZ* and *ACTB*) was assessed for all gene
49 variants (transcripts: XM_024446665.1 (**Figure 3B**), XM_017011752.2 (**Figure 3C**),
50 NM_001202483.2 (**Figure 3D**), NM_001202482.2 (**Figure 3E**), NM_001202481.1 (**Figure**
51 **3F**) and NM_001202475 (**Figure 3G**)); for all transcripts, abundance was not significantly
52 changed between groups.

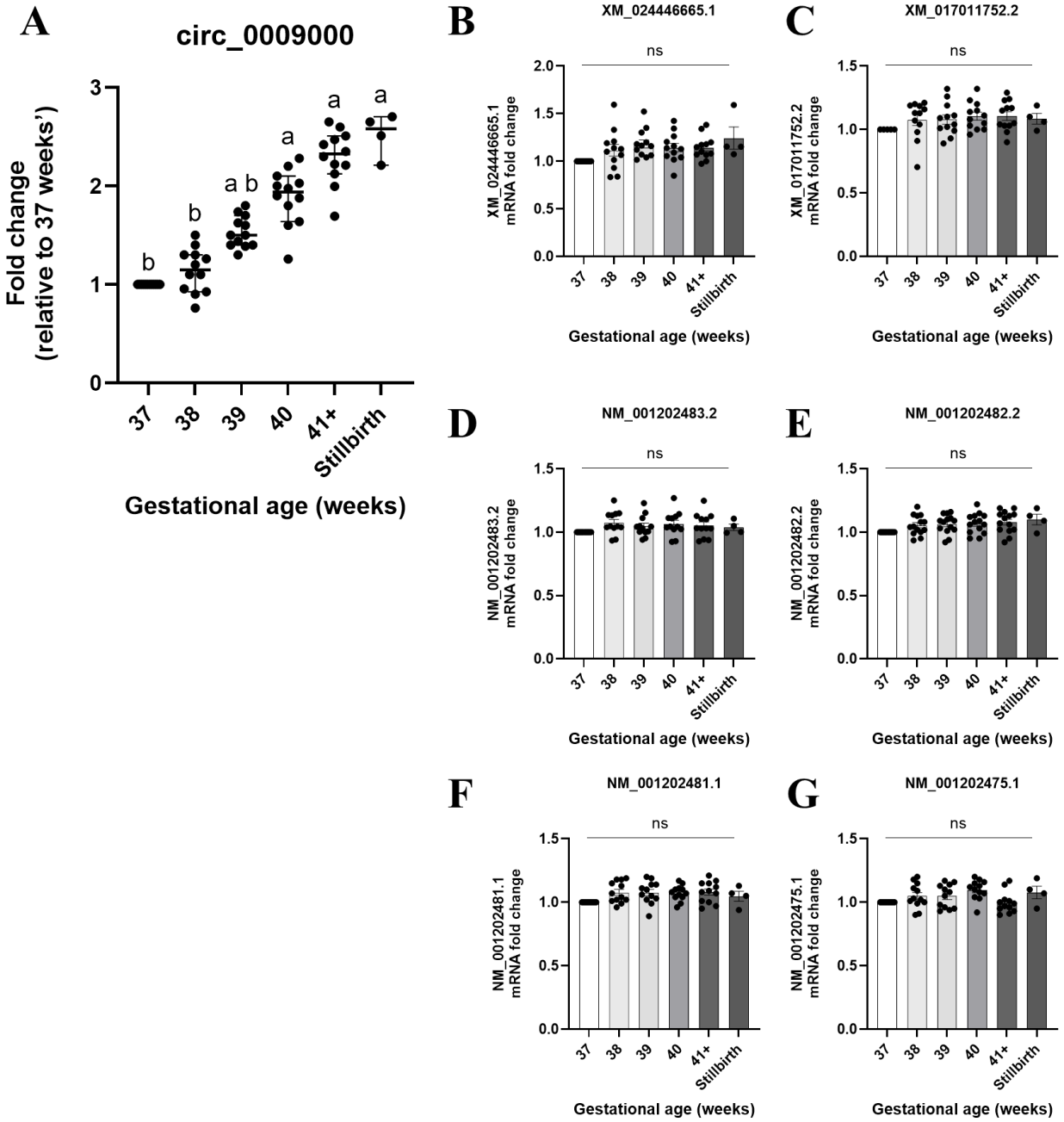

Figure 3. *Abundance (as fold change relative to abundance at 37 weeks' gestation) of* ***(A)*** *circ_0009000 and linear CRHR2 gene variants* ***(B)*** *XM_024446665.1,* ***(C)*** *XM_017011752.2,* ***(D)*** *NM_001202483.2,* ***(E)*** *NM_001202482.2,* ***(F)*** *NM_001202481.1 and* ***(G)*** *NM_001202475.1, in isolated cells from 37, 38, 39, 40 and 41+ uncomplicated, and stillbirth, placentae. n = 12 placentae / uncomplicated gestational group, n = 4 stillbirth placentae. Data are presented as scatter plots with bars, and indicate mean ± standard error of the mean. Different letters represent statistically significant (p < 0.05) differences. ns = not significant.*

54 **3.05 Abundance of circ_0024157, but not linear *CWF19L2* mRNA gene**
55 **variants, is increased in placentae from 40 and 41+ weeks' gestation, and in**
56 **stillbirth**

57 Relative abundance of circ_0024157, expressed as fold change on abundance levels in
58 placentae at 37 weeks' gestation, was significantly increased in cells from placentae sampled
59 at 40 weeks' gestation compared with 37 weeks' ($p = 0.0003$, **Figure 4A**). Relative abundance
60 was also increased in cells from placentae sampled at 41+ weeks' gestation compared with 37,
61 38 and 39 weeks' ($p_{37} < 0.0001$, $p_{38} = 0.0002$, $p_{39} = 0.0124$), as well as in placentae from
62 stillbirths compared with 37, 38 and 39 weeks' gestation ($p_{37} < 0.0001$, $p_{38} = 0.0027$, $p_{39} =$
63 0.0336).
64
65 Abundance of linear *CWF19L2* mRNA (relative to *YWHAZ* and *ACTB*) was assessed for all
66 gene variants (transcripts: XM_017017239.2 (**Figure 4B**), XR_947795.2 (**Figure 4C**),
67 NM_152434.3 (**Figure 4D**), and XM_011542620.3 (**Figure 4E**)); for all transcripts,
68 abundance was not significantly changed between groups.
69

70 **3.06 Abundance of circ_0061017, but not the linear *RAB22A* mRNA gene**
71 **variants, is increased in placentae from 39, 40 and 41+ weeks' gestation, and in**
72 **stillbirth**

73 Relative abundance of circ_0061017, expressed as fold change on abundance levels in
74 placentae at 37 weeks' gestation, was significantly increased in cells from placentae sampled
75 at 39 weeks' gestation compared with 37 weeks' ($p = 0.0260$; **Figure 4F**) and 40 weeks'
76 gestation compared with 37 and 38 weeks' ($p_{37} < 0.0001$, $p_{38} = 0.0053$). Relative abundance

77 was also increased in cells from placentae sampled at 41+ weeks' gestation compared with 37

78 and 38 weeks' ($p_{37} < 0.0001$, $p_{38} = 0.0003$), as well as in placentae from stillbirths compared

79 with 37 and 38 weeks' gestation ($p_{37} < 0.0001$, $p_{38} = 0.0034$).

80

81 Abundance of linear *RAB22A* mRNA (relative to *YWHAZ* and *ACTB*) was assessed for the only

82 gene variant (transcript: NM_020673.3 (**Figure 4G**); abundance was not significantly changed

83 between groups.

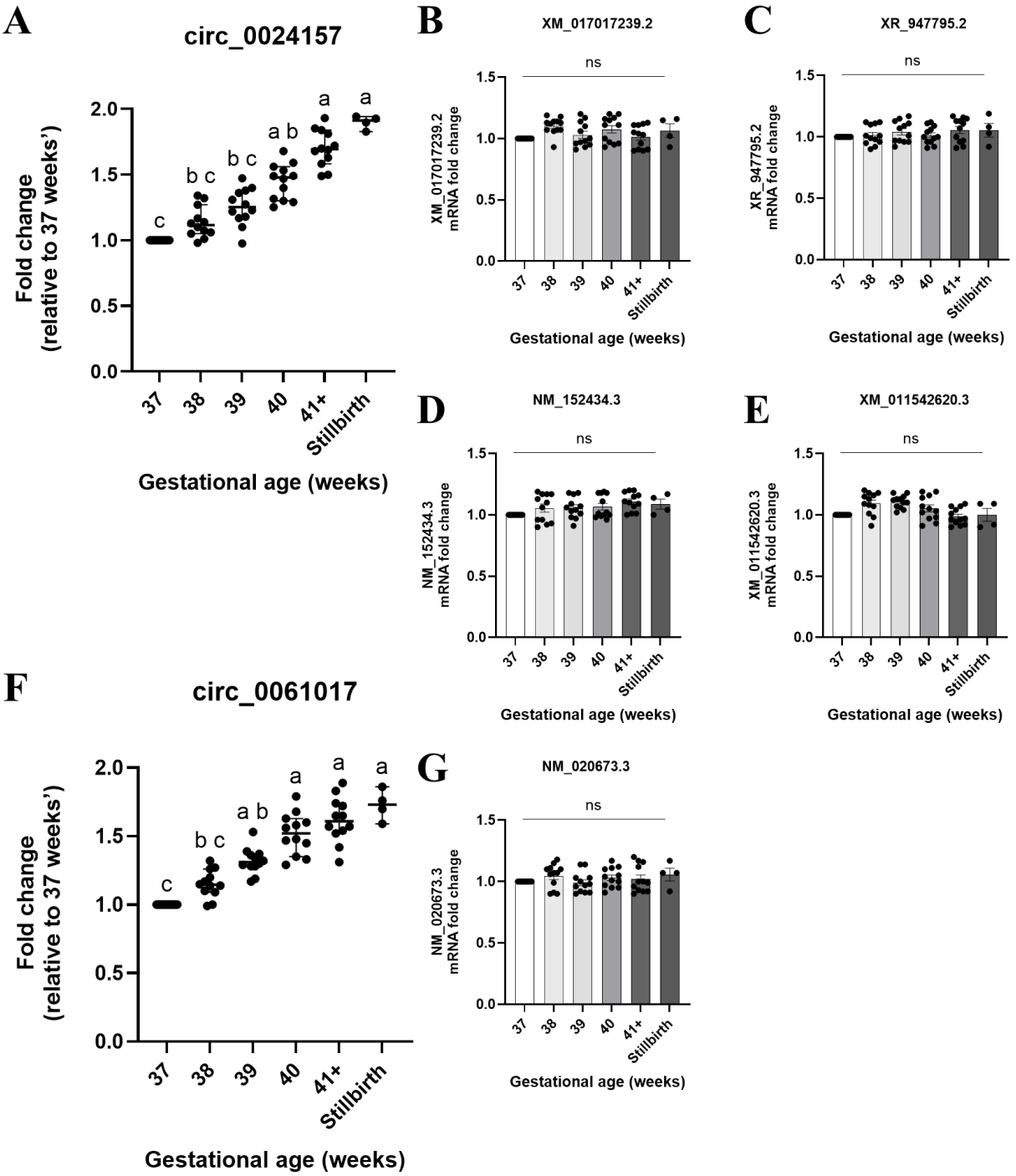

Figure 4. *Abundance (as fold change relative to abundance at 37 weeks' gestation) of* ***(A)*** *circ_0024157 and linear CWF19L2 gene variants* ***(B)*** *XM_017017239.2,* ***(C)*** *XR_947795.2,* ***(D)*** *NM_152434.3 and* ***(E)*** *XM_011542620.3. Abundance (as fold change relative to abundance at 37 weeks' gestation) of* ***(F)*** *circ_0061017 and linear RAB22A gene variant* ***(G)*** *NM_020673.3; all in isolated cells from 37, 38, 39, 40 and 41+ uncomplicated, and stillbirth, placentae. n = 12 placentae / uncomplicated gestational group, n = 4 stillbirth placentae. Data are presented as scatter plots with bars, and indicate mean ± standard error of the mean. Different letters represent statistically significant (p < 0.05) differences. ns = not significant.*

85 **3.07 Abundance of circ_0036877, but not linear *FURIN* mRNA gene variants,**
86 **is increased in placentae from 39, 40 and 41+ weeks' gestation, and in stillbirth**

87 Relative abundance of circ_0036877, expressed as fold change compared to abundance in
88 placentae at 37 weeks' gestation, was significantly increased in cells from placentae sampled
89 at 39 weeks' gestation compared with 37 weeks' (p = 0.0151; **Figure 5A**), and at 40 weeks'
90 gestation compared with 37 weeks' (p = 0.0002). circ_0036877 abundance was significantly
91 increased in cells from placentae taken at 41+ weeks' gestation compared with 37 and 38
92 weeks' (all $p < 0.0001$), as well as in placentae from stillbirths compared with 37 and 38 weeks'
93 gestation ($p_{37} < 0.0001$, $p_{38} = 0.0038$).
94
95 Abundance of linear *FURIN* mRNA (relative to *YWHAZ* and *ACTB*) was assessed for all gene
96 variants (transcripts: NM_001382622.1 (**Figure 5B**), NM_002569.4 (**Figure 5C**),
97 NM_001382619.1 (**Figure 5D**), NM_001289823.2 (**Figure 5E**), NR_168464.1 (**Figure 5F**)
98 NM_001382620.1 (**Figure 5G**), NM_001382621.1 (**Figure 5H**) and NM_001289824.2
99 (**Figure 5I**)); for all transcripts, abundance was not significantly changed between groups.
100

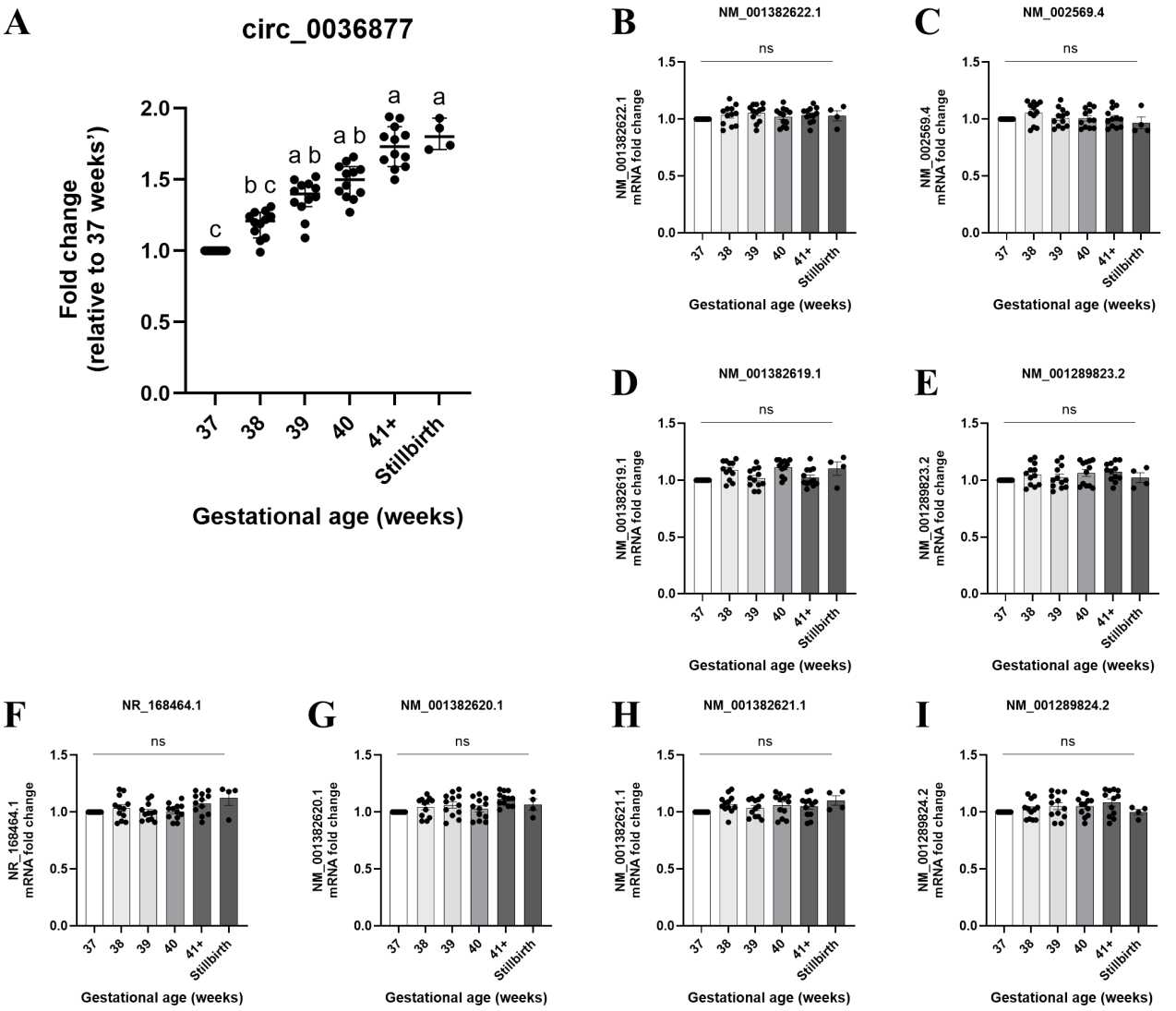

Figure 5. *Abundance (as fold change relative to abundance at 37 weeks' gestation) of* ***(A)*** *circ_0036877 and linear FURIN gene variants* ***(B)*** *NM_001382622.1,* ***(C)*** *NM_002569.4,* ***(D)*** *NM_001382619.1,* ***(E)*** *NM_001289823.2,* ***(F)*** *NR_168464.1,* ***(G)*** *NM_001382620.1,* ***(H)*** *NM_001382621.1 and* ***(I)*** *NM_001289824.2 in isolated cells from 37, 38, 39, 40 and 41+ uncomplicated, and stillbirth, placentae. n = 12 placentae / uncomplicated gestational group, n = 4 stillbirth placentae. Data are presented as scatter plots with bars, and indicate mean ± standard error of the mean. Different letters represent statistically significant (p < 0.05) differences. ns = not significant.*

101

102

103 **3.08 Abundance of circ_0054624, but not the linear *PNPT1* mRNA gene, is**
104 **increased in placentae from 40 and 41+ weeks' gestation, and in stillbirth**

105 Relative abundance of circ_0054624, expressed as fold change compared to abundance in
106 placentae at 37 weeks' gestation, was significantly increased in cells from placentae sampled
107 at 40 weeks' gestation compared with 37 and 38 weeks' ($p_{37} < 0.0001$, $p_{38} = 0.0232$; **Figure**
108 **6A**). circ_0054624 abundance was significantly increased in cells from placentae taken at 41+
109 weeks' gestation compared with 37, 38 and 39 weeks' ($p_{37} < 0.0001$, $p_{38} < 0.0001$, $p_{39} =$
110 0.0138), as well as in placentae from stillbirths compared with 37 and 38 weeks' gestation (p_{37}
111 < 0.0001, $p_{38} = 0.0012$).
112
113 Abundance of linear *PNPT1* mRNA (relative to *YWHAZ* and *ACTB*) was assessed for the only
114 gene variant (transcript: NM_033109.5 (**Figure 6B**)); abundance was not significantly changed
115 between groups.
116

117 **3.09 Abundance of circ_0111277, but not the linear *PAPPA2* mRNA gene, is**
118 **increased in placentae from 39, 40 and 41+ weeks' gestation, and in stillbirth**

119 Relative abundance of circ_0111277, expressed as fold change compared to abundance in
120 placentae at 37 weeks' gestation, was significantly increased in cells from placentae sampled
121 at 39 weeks' gestation compared with 37 weeks' ($p = 0.0443$; **Figure 6C**) and in cells from
122 placentae sampled at 40 weeks' gestation compared with 37 weeks' ($p = 0.0002$. circ_0111277
123 abundance was significantly increased in cells from placentae taken at 41+ weeks' gestation
124 compared with 37, 38 and 39 weeks' ($p_{37} < 0.0001$, $p_{38} < 0.0001$, $p_{39} = 0.0158$), as well as in

125 placentae from stillbirths compared with 37 and 38 weeks' gestation ($p_{37} < 0.0001$, $p_{38} =$

126 0.0042).

127

128 Abundance of linear *PAPPA2* mRNA (relative to *YWHAZ* and *ACTB*) was assessed for the

129 only gene variant (transcript: XM_005245422.3 (**Figure 6D**)); abundance was not significantly

130 changed between groups.

131

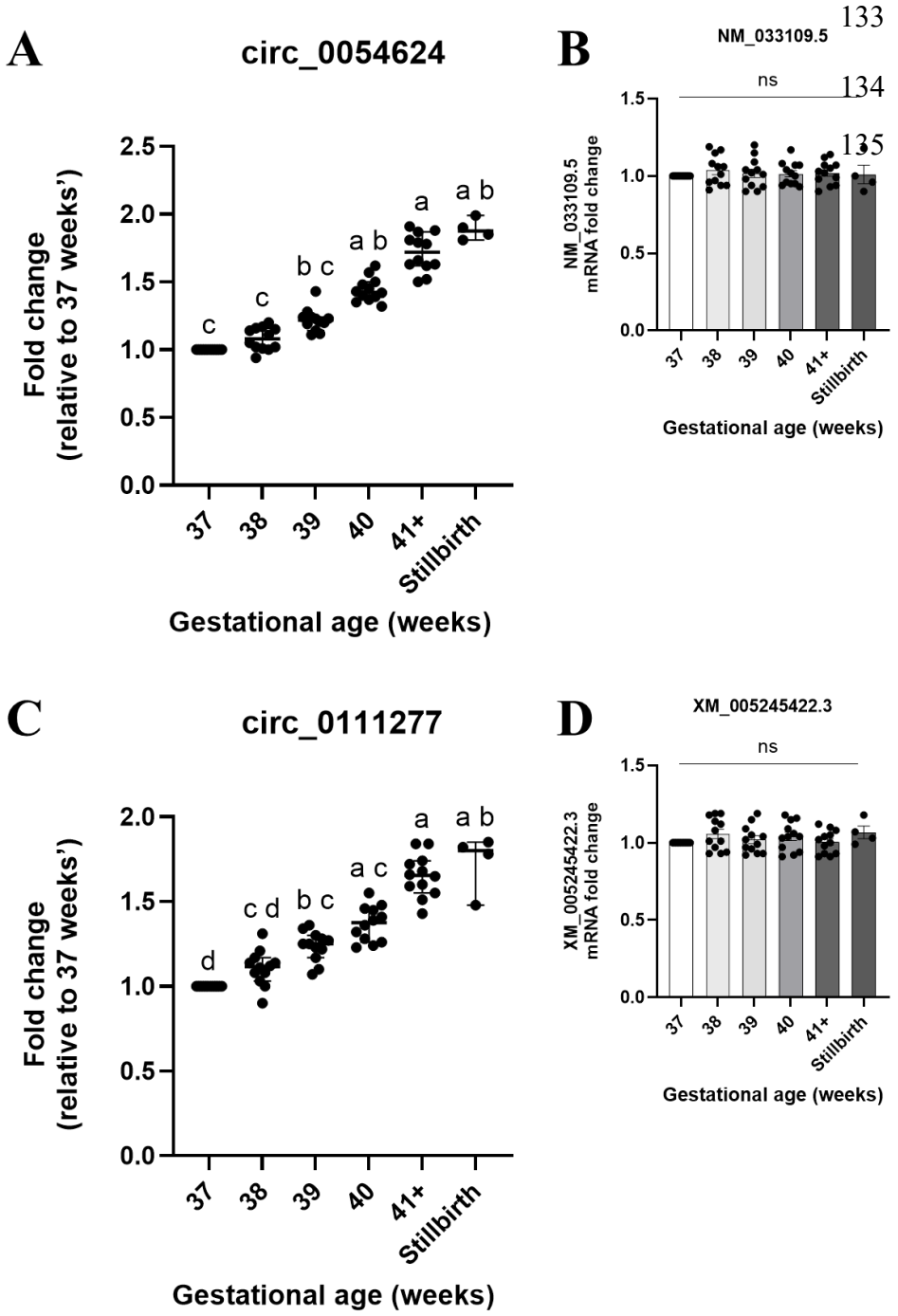

Figure 6. *Abundance (as fold change relative to abundance at 37 weeks' gestation) of* ***(A)*** *circ_0054624 and linear PNPT1 gene variant* ***(B)*** *NM_033109.5. Abundance (as fold change relative to abundance at 37 weeks' gestation) of* ***(C)*** *circ_0111277 and linear PAPPA2 gene variant* ***(D)*** *XM_005245422.3; all in isolated cells from 37, 38, 39, 40 and 41+ uncomplicated, and stillbirth, placentae. n = 12 placentae / uncomplicated gestational group, n = 4 stillbirth placentae. Data are presented as scatter plots with bars, and indicate mean ± standard error of the mean. Different letters represent statistically significant (p < 0.05) differences. ns = not significant.*

136 **3.10 circRNAs circ_0009000, circ_0024157, circ_0061017, circ_0036877,**
137 **circ_0054624 and circ_0111277 bind to DNA to create circR-loops in term**
138 **placentae**

139 DRIP-qPCR was used to detect circR-loops (DNA:RNA complexes) in pooled samples of
140 gestations 37-41+ weeks', to determine whether circRNAs which accumulate in the ageing
141 placenta interact directly with DNA.
142
143 After completing DRIP (see Methods) DRIP-qPCR analysis was undertaken using either
144 predesigned primers[18] for known R-loop-positive loci *TFPT* and *CALM3*, and known R-loop-
145 negative locus *EGFR1neg*, or using custom-designed primers (sequences listed in Methods) to
146 target the backsplice junctions of circ_0009000, circ_0024157, circ_0061017, circ_0036877,
147 circ_0054624 and circ_0111277. All DRIP-qPCR analyses were completed both in samples
148 treated with and without RNase H treatment prior to DRIP. As RNase H cleaves the RNA of
149 RNA:DNA hybrids, it is expected that addition of RNase H to the sample will result in a
150 significantly suppressed R-loop signal and hence, a reduced DRIP-qPCR signal (functioning
151 as a negative control). This was confirmed in our results.
152
153 According to Sanz, *et al.*[18], R-loop positive loci are typically recovered with an efficiency
154 ranging from 1-15% of total input, whereas negative loci are typically recovered with values
155 of <0.1%. This was replicated in our results for placenta tissue **(Figure 7A)**, where *TFPT* (mean
156 11.499%, $p = 0.0008$) and *CALM3* (mean 8.644%, $p = 0.0009$) produced DRIP-qPCR signals,
157 shown as a % of total DRIP input, significantly larger than their RNase H-treated controls.
158 There was no significant difference between the DRIP-qPCR signals of *EGFR1neg* (mean
159 0.389%) with and without RNase H treatment.

DRIP-qPCR signal for circ_0009000 (mean 0.173%, $p < 0.0001$; **Figure 7B**), circ_0024157 (mean 0.166%, $p < 0.0001$), circ_0061017 (mean 0.172%, $p < 0.0001$), circ_0036877 (mean 0.169%, $p < 0.0001$), circ_0054624 (mean 0.173%, $p < 0.0001$) and circ_0024157 (mean 0.177%, $p < 0.0001$) was significantly larger than their RNase H-treated controls.

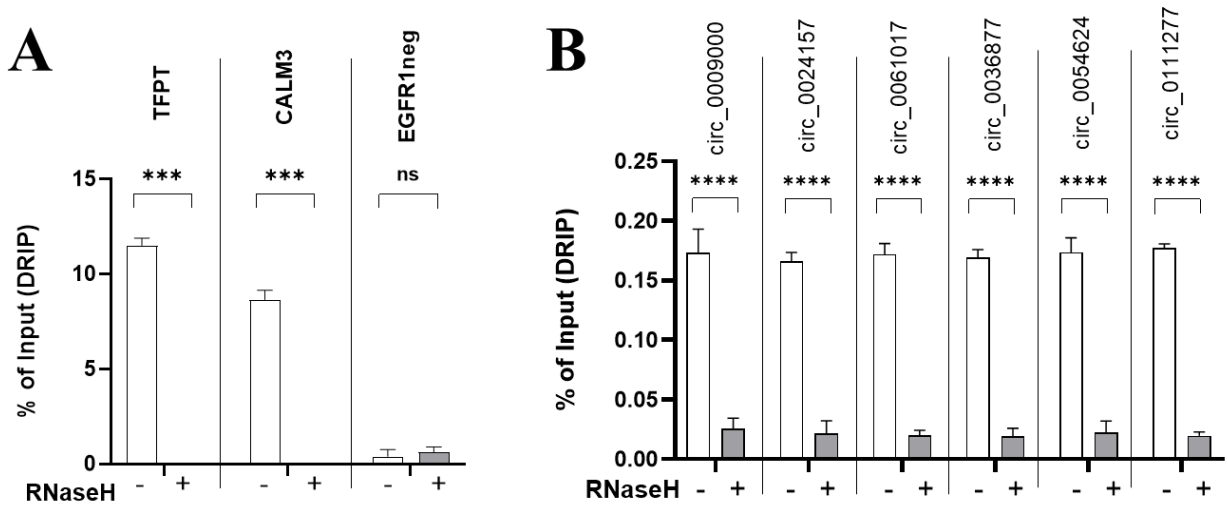

Figure 7. *DRIP-qPCR analysis using primers for* ***(A)*** *R-loop-positive loci TFPT and CALM3, and R-loop-negative locus EGFR1neg, and* ***(B)*** *circ_0009000, circ_0024157, circ_0061017, circ_0036877, circ_0054624 and circ_0111277. Where indicated, samples were treated with RNase H prior to DRIP. Treatment with RNase H significantly suppressed the DRIP-qPCR signal, consistent with R-loop formation in the tested regions. DRIP-qPCR signal intensity shown as % of Input (DRIP), with indication of mean ± standard error of the mean. *** $p < 0.001$, **** $p < 0.0001$, ns = not significant. n = 5 placentae with, and n = 5 placentae without, RNase H treatment.*

168 **3.11 DNA damage is mitigated with depletion of circ_0009000**

169 circR-loops introduce steric hinderance with the formation of the circRNA:DNA hybrid, which
170 can promote transcriptional pausing and subsequent DNA breaks[19-21], resulting in genomic
171 instability[22]. As such, we investigated whether circ_0009000, in forming a circR-loop, induces
172 DNA damage. This was confirmed using a custom-designed circ_0009000-specific siRNA in
173 HEK293T cells.

174

175 *Validation of the siRNA knockdown*

176 Cultured HEK293T cells were either untreated (control), treated with a scrambled siRNA or
177 with a custom-designed siRNA specific to circ_0009000. Cells were then cultured for 72 hours
178 prior to harvesting for qPCR analysis (**Figure 8A**) as well as Comet Assay analysis (**Figure**
179 **8B**).

180

181 As shown in **Figure 8A**, transfection with the scrambled siRNA did not alter the expression of
182 the linear *CRHR2* mRNA (shown as abundance relative to *YWHAZ* and *ACTB*) compared to
183 control. Importantly, administration of the siRNA specific to circ_0009000 did not alter the
184 expression of linear *CRHR2* mRNA. However, administration of the siRNA successfully
185 reduced the relative abundance of circ_0009000 compared with both the untreated cells
186 (control) and cells treated with the scrambled siRNA (all $p < 0.0001$).

187

188 *Quantification of DNA damage in circ_0009000-depleted HEK293T cells*

189 Transfection with the siRNA specific to circ_0009000 in HEK293T cells significantly reduced
190 the level of DNA damage (tail DNA%) compared with both the control (reduced by 41.3%)
191 and scrambled (reduced by 39.5%) groups (all $p < 0.0001$). Transfection with the scrambled

siRNA in HEK293T cells did not alter the level of DNA damage (tail DNA%) compared with the control, indicating that depletion of circ_0009000 results in reduced DNA damage.

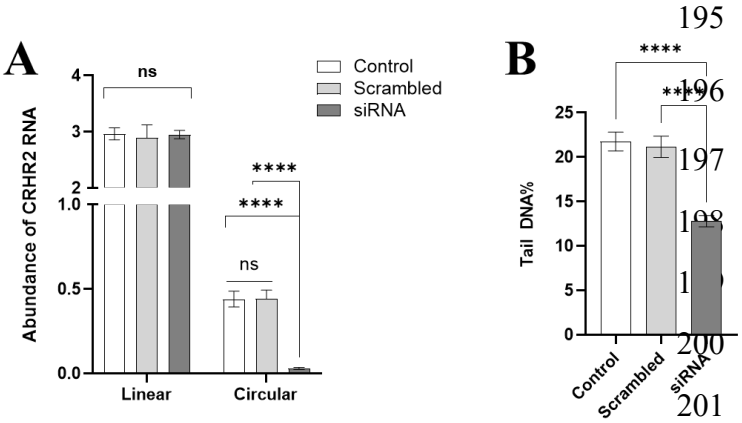

Figure 8. (A) *Abundance of CRHR2 mRNA ("linear") and circ_0009000 ("circular"), and* ***(B)*** *Levels of DNA damage, as assessed by Tail DNA %, in HEK293T cells, either untransfected ("control"), transfected with a scrambled siRNA ("scrambled") or transfected with an siRNA specific to circ_0009000 ("siRNA"). n = 9 / group. 100 cells analysed following Comet Assay, per group. Data are presented as mean ± standard error of the mean. **** $p < 0.0001$, ns = not significant.*

204 # 4. Discussion

205 Like other tissues in the body, the placenta undergoes the normal phenomenon of ageing.
206 Tissue ageing includes progressive increases in cellular senescence[23]. For the placenta, this
207 implies a decline in functionality as gestational age increases, resulting in a reduced capacity
208 of the placenta to support the fetus[3]. Placentae from stillbirths undergo an accelerated ageing
209 process[3], exhibiting similar pathological features regardless of their earlier gestational ages.
210 Markers of ageing such as increased DNA and RNA oxidation, lipid peroxidation, altered
211 perinuclear location of lysosomes and larger autophagosomes are found in placentae from
212 stillbirths as well as those from healthy late term compared with placentae from healthy early
213 term[3]. In this study we provide new and compelling evidence to support the notion of premature
214 placental ageing in stillbirth, as we found increased DNA breaks in placentae from stillbirths
215 and those from healthy late term (40, 41+ weeks' gestation) compared with those from early
216 term (37-39 weeks').
217
218 Our group 41+ weeks' gestation encompassed women who birthed between 41+1 and 41+6
219 weeks'. Given that gestation of >40 weeks, in addition to maternal age ≥35 years[3] and male
220 fetal sex[1], are risk factors for stillbirth, the Australian Pregnancy Care Guidelines consider 42
221 weeks' and beyond as post-term and recommend fetal monitoring and induction of labour from
222 41 weeks', even in uncomplicated, low risk patients[24]. Indeed, evidence shows that stillbirth
223 and neonatal death can be reduced with fetal surveillance twice weekly from 39 weeks'[25]. This
224 study confirmed that rates of DNA damage in placentae from 41+ weeks' gestation were
225 significantly increased compared to earlier term gestations. Placentae from stillbirths had
226 further elevated DNA damage, although this was not statistically significant from those at 41+
227 weeks' potentially due to the small sample size. As our stillbirth placentae were collected at
228 gestational weeks 23, 26, 31 and 34, and DNA damage is a recognised marker of tissue

229 ageing[26], this clearly indicates that in stillbirth the placenta experiences accelerated tissue
230 ageing, resulting in a post-term phenotype much earlier than would be appropriate for their
231 gestational age.
232
233 The accumulation of circRNAs in aged tissue is a relatively recent discovery. Preliminary
234 evidence for this was uncovered from RNA-seq libraries from *Drosophila melanogaster*, where
235 expression of >200 circRNAs were significantly increased in the heads of 20-day old flies,
236 compared with 1-day old flies[6]. Accumulation of circRNAs with ageing has also been evident
237 in studies[27] using *Drosophila melanogaster* photoreceptor neurons[28], mouse brain and heart[8]
238 and *Caenorhabditis elegans*[7]. It is most likely that circRNAs accumulate in tissues as their lack
239 of a 5' cap and polyadenylated tail renders them resistant to exoribonuclease degradation[29].
240 Another explanation for circRNA accumulation in some tissues is that in cell types such as
241 neurons, rates of mitosis and proliferation are lower than other cell types, allowing reduced
242 turnover of circRNAs[27,30-32]. Given that the nuclei of the syncytiotrophoblast are non-mitotic[33],
243 transcription is significantly reduced[34] and the syncytiotrophoblast displays markers of
244 senescence[35,36], this could be a primary area of circRNA accumulation.
245
246 Recently, circRNAs were identified as a potential forensic tool for estimating biological age
247 using a panel of 5 circRNAs which accumulate in human blood[37], which is an exciting leap
248 from circRNA accumulation in animals to differential circRNA expression with age in humans.
249 Other studies have shown differentially expressed circRNAs in human granulosa cells from
250 women who were young versus those of advanced reproductive age[38], and that specific
251 circRNAs in human peripheral blood were associated with parental longevity and cellular
252 senescence[39]. The link between circRNA differential expression and Alzheimer's disease is
253 becoming more widely investigated[40], which is of particular interest to this study given that

254 Alzheimer's disease is, at its core, an ageing disorder[41]. Whilst these studies demonstrate that
255 expression of circRNAs is *changed* between differently aged groups, none of these studies
256 investigated circRNAs *accumulation* in ageing tissue.
257
258 The abundance of a circRNA is a combination of expression level as well as accumulation.
259 circRNA expression level can be increased by overexpressing the linear gene, or by alternative
260 splicing that promotes the circular over the linear transcript(s). circRNA accumulation
261 indicates that the circRNA remains in the tissue[27], unaffected by exoribonucleases[29]. Over time,
262 the abundance of the circRNA in the tissue increases as the accumulated transcripts escape
263 degradation. This occurs without change in the linear gene expression nor alternative splicing.
264 The result is that these circRNAs can continually exert their function in the tissue well after
265 their linear gene's expression and at higher-than-expected abundance.
266
267 As an organ that undergoes a well-characterised ageing process during gestation, we
268 hypothesised that the placenta may also experience circRNA accumulation with tissue ageing.
269 In this study, we report the first evidence of circRNA accumulation in human tissue. circRNAs
270 circ_0009000, circ_0024157, circ_0061017, circ_0036877, circ_0054624 and circ_0111277
271 were all increased in abundance in human placentae from late term (40, 41+ weeks') compared
272 with early term (37, 38, 39 weeks'), while abundance of their cognate linear mRNAs were
273 unchanged. Furthermore, we found no evidence of changed alternative splicing patterns, as
274 indicated by absence of differential expression of gene variants between gestational weeks.
275 This indicates that the excess levels of these candidate circRNAs found in late term compared
276 with early term placentae were not the product of increased gene expression, nor the product
277 of a switch to a different dominant isoform of the gene which may result in production of a
278 circular transcript. Hence, we can conclude that these candidate circRNAs accumulate in the
279 tissue as gestation continues and the organ ages.

280

281 To our knowledge, ours is the first study to confirm that circRNAs accumulate in human aged
282 tissue. Importantly, we established that there is no global increase in total RNA, nor circular
283 RNA, abundance with placental gestational age. This confirms that our candidate circRNAs
284 are unique in their ability to accumulate with age. It should be noted that accumulation of these
285 specific circRNAs with age may be placenta-specific, as this study only examined placental
286 tissue, and this candidate list may not be exhaustive. Further studies will profile all
287 accumulating circRNAs in the placenta as it ages.

288

289 Due to the low abundance of the candidate circRNAs, we investigated their interaction with
290 DNA as a stoichiometrically favourable potential function (given that there are only 2 copies
291 of DNA per cell, compared with thousands of microRNAs and proteins). By performing DRIP
292 on RNA which was later treated with RNase R to degrade linear transcripts, this allowed
293 isolation of circRNA moieties that bind placental DNA. DRIP-qPCR analysis showed that
294 circRNAs circ_0009000, circ_0024157, circ_0061017, circ_0036877, circ_0054624 and
295 circ_0111277, which accumulate with gestational age and in stillbirth, also form circR-loops
296 in term placentae.

297

298 A circR-loop is formed when a circRNA molecule binds one strand of helicase-unwound
299 genomic DNA[10]. The steric hindrance of this bulky structure causes RNA polymerase II to stall
300 during transcription, resulting in a DNA break, and often a subsequent fusion at another locus[42],
301 promoting genomic instability[11]. Double-stranded DNA breaks are lethal to cells, as they affect
302 both strands of DNA and promote the loss of genetic information[13]. Any type of DNA damage
303 can trigger cellular apoptosis or senescence[12]. Given that we observed increased DNA breaks
304 in stillbirth placentae, which also had elevated abundance of circ_0009000, we utilised a

305 circ_0009000 knockdown model in HEK293T cells to determine whether presence of this
306 circRNA was associated with induction of DNA damage.
307
308 Results from this study indicate that targeted knockdown of circ_0009000 with an siRNA
309 reduces double-stranded DNA damage in HEK293T cells. Importantly, this occurred in the
310 absence of any change in the linear mRNA expression, indicating that this is a circRNA-
311 specific result. While this finding does not elucidate a molecular mechanism for circ_0009000
312 induction of DNA damage, nor does it indicate that this occurs in the human placenta *in vivo*,
313 it provides compelling evidence to further support the hypothesis that circ_0009000 causes
314 DNA breaks by forming circR-loops with placental DNA. This represents an important avenue
315 for further investigation, with therapeutic potential in reducing circRNAs accelerating
316 placental ageing. Indeed, the use of, and targeted inhibition of, circRNAs as a therapeutic
317 option is growing[43-46].
318
319 circ_0009000 is formed by non-canonical splicing of *CRHR2*, the gene for corticotrophin
320 releasing hormone receptor 2 (CRHR2). Corticotrophin releasing hormone (CRH) production
321 in the placenta is largely in the second and third trimesters of pregnancy[47], with CRH playing
322 a critical role in parturition. Most CRH is secreted into the maternal bloodstream[48], however
323 CRH receptors 1 (CRHR1) and 2 (CRHR2) (and their various isoforms) can be found in the
324 placenta, with immunohistochemical staining localising CRHR2 mainly to the
325 syncytiotrophoblast[49]. As circ_0009000 forms a circR-loop in placenta, binding its cognate
326 locus, it is possible that this inhibits the translation of *CRHR2*, reducing availability of CRHR2
327 for CRH binding. Indeed, one study noted a significant downregulation in *CRH* mRNA
328 expression in placentae from idiopathic stillbirths compared with live births[50], implying that

329 *CRH* mRNA may be downregulated to produce less CRH protein, which coheres with reduced
330 availability of CRHR2 for binding.
331
332 Many other circRNAs this study confirmed to form circR-loops in placenta were also from
333 genes that encode important proteins in placental function and pregnancy. *FURIN* encodes a
334 pro-protein convertase that facilitates placental syncytialisation in first trimester trophoblasts[51],
335 and *PAPPA2* encodes a metalloproteinase which cleaves Insulin Growth Factor (IGF) Binding
336 Protein-3 and -5 (IGFBR3, IGFBP5), liberating IGF-1 for binding to membrane receptors[52].
337 Further investigations should assess whether circ_0036877 and circ_0111277 (from *FURIN*
338 and *PAPPA2*, respectively) binding at their cognate loci reduce production of their respective
339 encoded proteins. Indeed, there is evidence to suggest that FURIN is mainly associated with
340 functions in early gestation[53]. Conversely, abnormally low PAPPA2 expression at term is
341 associated with fetal growth restriction in humans[54], and *PAPPA2* knockout mice experience
342 postnatal growth retardation and elevated total IGF-1[55].
343
344 To summarise, this study provides evidence that (a) multiple circRNAs accumulate in human
345 aged placental tissue and stillbirth placentae, (b) these circRNAs bind to DNA in the human
346 term placenta to form circR-loops and (c) circ_0009000 has the capacity to facilitate DNA
347 damage in human cells. We propose the following mechanism as a potential contributor to
348 stillbirth pathology (**Figure 9**): In uncomplicated pregnancy, circRNAs naturally accumulate
349 in placental cells as the tissue ages with gestation. However, in pregnancies resulting in
350 unexplained stillbirth, premature placental ageing results in accelerated accumulation of
351 circRNAs. These circRNAs form circRNA:DNA complexes in the placenta, with at least one
352 circRNA (circ_0009000) known to facilitate DNA damage. As DNA breaks facilitate genomic

353 instability[11] and cellular senescence[56] and apoptosis[57], this may result in reducing placental
354 function to the detriment of the fetus.
355

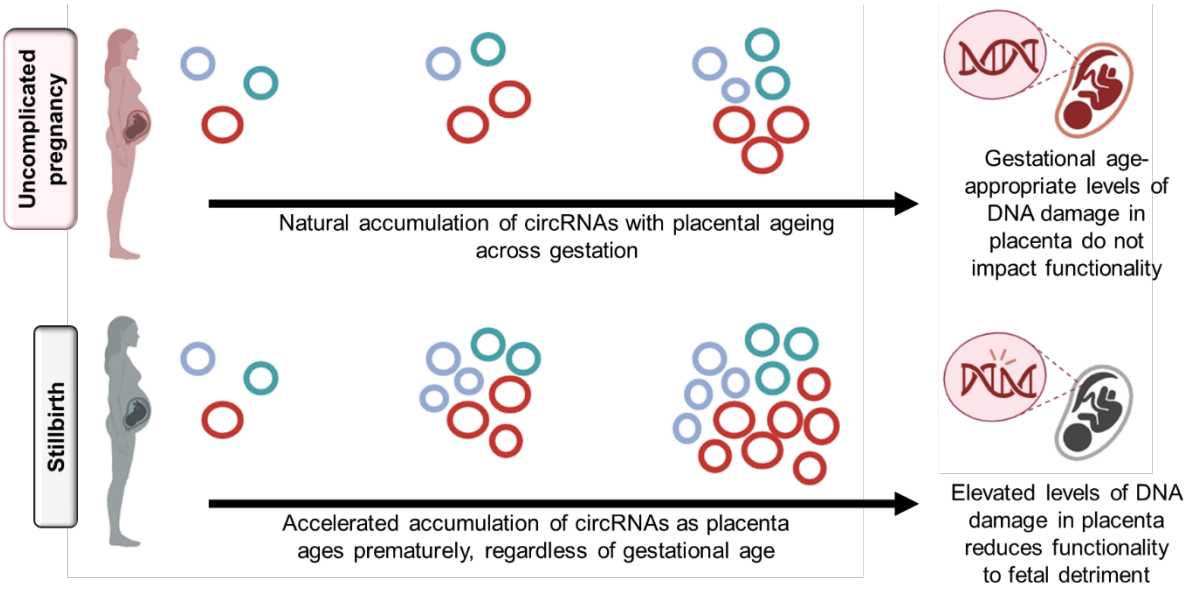

Figure 9. *Proposed mechanism by which circRNA accumulation and placental ageing contribute to stillbirth.*

356

357 A limitation of this study is the small sample size of stillbirth placentae; however, this is a
358 common issue in stillbirth research[3,58] given the difficulty in obtaining tissue within an
359 appropriate timeframe. As stillbirths that could be explained by fetal congenital abnormality
360 were excluded, resulting in a pure "unexplained stillbirth" sample pool, this further reduced
361 available tissue samples. Moreover, sample size limited our ability to perform fetal sex-specific
362 statistical tests. Further studies will be conducted with larger sample sizes to allow for increased
363 comparisons. Future studies will also include participants of different ethnicities, accounting
364 for ethnicities which are more prone to stillbirths (such as South Asian women[25]).
365

366 Here, we present the first report of circRNA accumulation in ageing human placental tissue, in
367 the absence of any change in total linear or circular RNA expression nor alternative splicing

368 variants. Importantly, circRNAs circ_0009000, circ_0024157, circ_0061017, circ_0036877,
369 circ_0054624 and circ_0111277 are present at exceptionally high levels in placenta from
370 stillbirths, similar to or surpassing the circRNA levels found in post-term placentae.
371 Furthermore, our study provides evidence that these circRNAs bind to DNA to form circR-
372 loops in placental tissue. Finally, our *in vitro* experiments show that knockdown of
373 circ_0009000 results in decreased DNA breaks in cells, indicating that this circRNA facilitates
374 DNA damage.
375

Author Contributions

A.L.A. conceptualised this work, performed experimental work and formal analysis of data, original draft preparation, and review and editing. M.R.J., H.S.S. and C.P.B. provided stillbirth placenta samples and reviewed and edited the manuscript. D.M. contributed to experimental work and data analysis. S.W. provided molecular expertise and reviewed and edited the manuscript. M.D.S. and T.J-K. reviewed and edited the manuscript. G.A.D. provided clinical expertise and reviewed and edited the manuscript. C.T.R. provided supervision, funding acquisition, interpretation of data, review and editing of the manuscript. All authors contributed to the article and approved the final version.

Funding

A.L.A. is supported by funding from the Flinders Foundation, Flinders University and the Channel 7 Children's Research Foundation.

C.T.R. is supported by an NHMRC Investigator Grant (GNT1174971) and a Matthew Flinders Fellowship from Flinders University.

The Genomic Autopsy Study was supported by NHMRC (#APP1123341), Genomics Health Futures Mission – Medical Research Futures Fund (#GHFM76777) and the Australian Genomic Health Alliance NHMRC Targeted Call for Research into Preparing Australia for the Genomics Revolution in Healthcare (#GNT1113531) to H.S.S. and C.P.B.

Conflict of Interest

Provisional patent #1297095, filed 2nd September 2024.

Acknowledgments

We thank the women who consented to their placental tissue being used for this research. Thank you to the clinical and anatomical staff from the Women's and Children's Hospital and Lyell McEwin Hospital who were involved in the women's care, and who collected and biopsied the placental samples.

Figures were created using Biorender.com

References

1 Australian Institute of Health and Welfare, 2018.

2 Hug, L., You, D., Blencowe, H., Mishra, A., Wang, Z. *et al.* Global, regional, and national estimates and trends in stillbirths from 2000 to 2019: a systematic assessment. *The Lancet* **398**, 772-785 (2021).

3 Maiti, K., Sultana, Z., Aitken, R. J., Morris, J., Park, F. *et al.* Evidence that fetal death is associated with placental aging. *Am J Obstet Gynecol* **217**, 441 (2017).

4 Amir, H., Weintraub, A., Aricha-Tamir, B., Apel-Sarid, L., Holcberg, G. *et al.* A piece in the puzzle of intrauterine fetal death: pathological findings in placentas from term and preterm intrauterine fetal death pregnancies. *The journal of maternal-fetal & neonatal medicine* **22**, 759-764 (2009).

5 Ferrari F, F. F., Saade G, Menon R. Placental telomere shortening in stillbirth: a sign of premature senescence? *Journal of Maternal-Fetal and Neonatal Medicine* **29**, 1283-1288 (2016).

6 Westholm, J. O., Miura, P., Olson, S., Shenker, S., Joseph, B. *et al.* Genome-wide analysis of drosophila circular RNAs reveals their structural and sequence properties and age-dependent neural accumulation. *Cell reports* **9**, 1966-1980 (2014).

7 Cortes-Lopez M, G. M., Cooper DA, Gruner HN, Voda AI, van der Linden AM, Miura P. Global accumulation of circRNAs during aging in Caenorhabditis elegans. *BMC Genomics* **19** (2018).

8 Gruner H, C.-L. M., Cooper DA, Bauer M, Miura P. . CircRNA accumulation in the aging mouse brain. *Sci Rep* **6**, 38907 (2016).

9 Arthurs, A. L., Jankovic-Karasoulos, T., Smith, M. D. & Roberts, C. T. Circular RNAs in Pregnancy and the Placenta. *International Journal of Molecular Sciences* **23**, 4551 (2022).

10 Conn, S. J., Pillman, K. A., Toubia, J., Conn, V. M., Salmanidis, M. *et al.* The RNA binding protein quaking regulates formation of circRNAs. *Cell* **160**, 1125-1134 (2015).

11 Lord, C. J. & Ashworth, A. The DNA damage response and cancer therapy. *Nature* **481**, 287-294 (2012).

12 Parrinello, S., Coppe, J.-P., Krtolica, A. & Campisi, J. Stromal-epithelial interactions in aging and cancer: senescent fibroblasts alter epithelial cell differentiation. *Journal of cell science* **118**, 485-496 (2005).

13 Altaf, M., Saksouk, N. & Côté, J. Histone modifications in response to DNA damage. *Mutation Research/Fundamental and Molecular Mechanisms of Mutagenesis* **618**, 81-90 (2007).

14 Mohammed, H., Roberts, C. T., Grzeskowiak, L. E., Giles, L. C., Dekker, G. A. *et al.* Safety and protective effects of maternal influenza vaccination on pregnancy and birth outcomes: A prospective cohort study. *EClinicalMedicine* **26**, 100522 (2020).

15 Byrne, A. B., Arts, P., Ha, T. T., Kassahn, K. S., Pais, L. S. *et al.* Genomic autopsy to identify underlying causes of pregnancy loss and perinatal death. *Nature Medicine* **29**, 180-189 (2023).

16 Drula, R., Braicu, C., Chira, S. & Berindan-Neagoe, I. Investigating circular RNAs using qRT-PCR; roundup of optimization and processing steps. *International Journal of Molecular Sciences* **24**, 5721 (2023).

17 Livak, K. J. & Schmittgen, T. D. Analysis of relative gene expression data using real-time quantitative PCR and the $2^{-\Delta\Delta CT}$ method. *methods* **25**, 402-408 (2001).

18 Sanz, L. A. & Chédin, F. High-resolution, strand-specific R-loop mapping via S9. 6-based DNA–RNA immunoprecipitation and high-throughput sequencing. *Nature protocols* **14**, 1734-1755 (2019).
19 El Hage, A., Webb, S., Kerr, A. & Tollervey, D. Genome-wide distribution of RNA-DNA hybrids identifies RNase H targets in tRNA genes, retrotransposons and mitochondria. *PLoS genetics* **10**, e1004716 (2014).
20 Alexander, R. D., Innocente, S. A., Barrass, J. D. & Beggs, J. D. Splicing-dependent RNA polymerase pausing in yeast. *Molecular cell* **40**, 582-593 (2010).
21 Wongsurawat, T., Jenjaroenpun, P., Kwoh, C. K. & Kuznetsov, V. Quantitative model of R-loop forming structures reveals a novel level of RNA–DNA interactome complexity. *Nucleic acids research* **40**, e16-e16 (2012).
22 Conn, V. M., Gabryelska, M., Toubia, J., Kirk, K., Gantley, L. *et al.* Circular RNAs drive oncogenic chromosomal translocations within the MLL recombinome in leukemia. *Cancer cell* **41**, 1309-1326. e1310 (2023).
23 Holt, D., Grainger, DW. Senescence and quiescence induced compromised function in cultured macrophages. *Biomaterials* **33**, 7497-7507 (2012).
24 Australian_Government_Department_of_Health. (ed Department of Health) (Canberra, 2020).
25 Davies-Tuck, M. L., Davey, M.-A., Hodges, R. L. & Wallace, E. M. Fetal surveillance from 39 weeks' gestation to reduce stillbirth in South Asian-born women. *American Journal of Obstetrics and Gynecology* **229**, 286. e281-286. e289 (2023).
26 Schumacher, B., Pothof, J., Vijg, J. & Hoeijmakers, J. H. The central role of DNA damage in the ageing process. *Nature* **592**, 695-703 (2021).
27 Knupp, D. & Miura, P. CircRNA accumulation: A new hallmark of aging? *Mech Ageing Dev* **173**, 71-79 (2018).
28 Hall H, M. P., Cooper DA. et al. . Transcriptome profiling of aging Drosophila photoreceptors reveals gene expression trends that correlate with visual senescence. *BMC Genomics* **18** (2017).
29 Jeck, W., Sorrentino, J., Wang, K., Slevin, M., Burd, C. *et al.* Circular RNAs are abundant, conserved, and associated with ALU repeats. *RNA* **19**, 141-157 (2013).
30 Rybak-Wolf, A., Stottmeister, C., Glažar, P., Jens, M., Pino, N. *et al.* Circular RNAs in the mammalian brain are highly abundant, conserved, and dynamically expressed. *Molecular cell* **58**, 870-885 (2015).
31 Bachmayr-Heyda, A., Reiner, A. T., Auer, K., Sukhbaatar, N., Aust, S. *et al.* Correlation of circular RNA abundance with proliferation–exemplified with colorectal and ovarian cancer, idiopathic lung fibrosis and normal human tissues. *Scientific reports* **5**, 8057 (2015).
32 Song, X., Zhang, N., Han, P., Moon, B.-S., Lai, R. K. *et al.* Circular RNA profile in gliomas revealed by identification tool UROBORUS. *Nucleic acids research* **44**, e87-e87 (2016).
33 Mayhew, T. & Simpson, R. Quantitative evidence for the spatial dispersal of trophoblast nucleic in human placental villi during gestation. *Placenta* **15**, 837-844 (1994).
34 Huppertz, B., Frank, H.-G., Reister, F., Korr, H. & Kaufmann, P. Apoptosis cascade progresses during turnover of human trophoblast: analysis of villous cytotrophoblast and syncytial fragments in vitro. *Laboratory investigation; a journal of technical methods and pathology* **79**, 1687-1702 (1999).
35 Chuprin, A., Gal, H., Biron-Shental, T., Biran, A., Amiel, A. *et al.* Cell fusion induced by ERVWE1 or measles virus causes cellular senescence. *Genes & development* **27**, 2356-2366 (2013).

36 Goldman-Wohl, D. & Yagel, S. United we stand not dividing: the syncytiotrophoblast and cell senescence. *Placenta* **35**, 341-344 (2014).
37 Wang, J., Wang, C., Wei, Y., Zhao, Y., Wang, C. *et al.* Circular RNA as a potential biomarker for forensic age prediction. *Frontiers in Genetics* **13**, 29 (2022).
38 Cheng, J., Huang, J., Yuan, S., Zhou, S., Yan, W. *et al.* Circular RNA expression profiling of human granulosa cells during maternal aging reveals novel transcripts associated with assisted reproductive technology outcomes. *PLoS ONE* **12**, e0177888 (2017).
39 Haque, S., Ames, R. M., Moore, K., Pilling, L. C., Peters, L. L. *et al.* circRNAs expressed in human peripheral blood are associated with human aging phenotypes, cellular senescence and mouse lifespan. *GeroScience* **42**, 183-199 (2020).
40 Akhter, R. in *Circular RNAs* (ed J Xiao) (Springer Nature, 2018).
41 Smith, M. A., Sayre, L. M., Monnier, V. M. & Perry, G. Radical AGEing in Alzheimer's disease. *Trends in neurosciences* **18**, 172-176 (1995).
42 Conn, V. M., Hugouvieux, V., Nayak, A., Conos, S. A., Capovilla, G. *et al.* A circRNA from SEPALLATA3 regulates splicing of its cognate mRNA through R-loop formation. *Nature Plants* (2017).
43 Sun, M. & Yang, Y. Biological functions and applications of circRNAs-next generation of RNA-based therapy. *J Mol Cell Biol* **15** (2023).
44 Woodruff, R., Parekh, F., Lamb, K., Mekkaoui, L., Allen, C. *et al.* Large-scale manufacturing of base-edited chimeric antigen receptor T cells. *Mol Ther Methods Clin Dev* **31**, 101123 (2023).
45 Shen, L., Yang, J., Zuo, C., Xu, J., Ma, L. *et al.* Circular mRNA-based TCR-T offers a safe and effective therapeutic strategy for treatment of cytomegalovirus infection. *Mol Ther* **32**, 168-184 (2024).
46 He, A. T., Liu, J., Li, F. & Yang, B. B. Targeting circular RNAs as a therapeutic approach: current strategies and challenges. *Signal Transduction and Targeted Therapy* **6**, 185 (2021).
47 Frim, D., Emanuel, R., Robinson, B., Smas, C., Adler, G. *et al.* Characterization and gestational regulation of corticotropin-releasing hormone messenger RNA in human placenta. *The Journal of clinical investigation* **82**, 287-292 (1988).
48 Campbell, E., Linton, E., Wolfe, C., Scraggs, P., Jones, M. *et al.* Plasma corticotropin-releasing hormone concentrations during pregnancy and parturition. *The Journal of Clinical Endocrinology & Metabolism* **64**, 1054-1059 (1987).
49 Sehringer, B., Zahradnik, H., Simon, M., Ziegler, R., Noethling, C. *et al.* mRNA expression profiles for corticotrophin-releasing hormone, urocortin, CRH-binding protein and CRH receptors in human term gestational tissues determined by real-time quantitative RT-PCR. *Journal of molecular endocrinology* **32**, 339-348 (2004).
50 Vasconcelos, S., Moustakas, I., Branco, M. R., Guimarães, S., Caniçais, C. *et al.* Syncytiotrophoblast Markers Are Downregulated in Placentas from Idiopathic Stillbirths. *International Journal of Molecular Sciences* **25**, 5180 (2024).
51 Zhou, Z., Zhang Q, Lu X, Wang R, Wang H, Wang Y-L, Zhu C, Lin H-Y, Wang H. The proprotein convertase furin is required for trophoblast syncytialization. *Cell Death and Disease* **4**, e593 (2013).
52 Overgaard, M. T., Boldt, H. B., Laursen, L. S., Sottrup-Jensen, L., Conover, C. A. *et al.* Pregnancy-associated plasma protein-A2 (PAPP-A2), a novel insulin-like growth factor-binding protein-5 proteinase. *Journal of Biological Chemistry* **276**, 21849-21853 (2001).

53 Morosin, S. K., Delforce, S. J., Corbisier de Meaultsart, C., Lumbers, E. R. & Pringle, K. G. FURIN and placental syncytialisation: a cautionary tale. *Cell Death & Disease* **12**, 635 (2021).

54 Dauber, A., Muñoz-Calvo, M. T., Barrios, V., Domené, H. M., Kloverpris, S. *et al.* Mutations in pregnancy associated plasma protein A2 cause short stature due to low IGF-I availability. *EMBO Molecular Medicine* **8**, 363-374 (2016).

55 Conover, C. A., Boldt, H. B., Bale, L. K., Clifton, K. B., Grell, J. A. *et al.* Pregnancy-associated plasma protein-A2 (PAPP-A2): tissue expression and biological consequences of gene knockout in mice. *Endocrinology* **152**, 2837-2844 (2011).

56 McHugh, D. & Gil, J. Senescence and aging: Causes, consequences, and therapeutic avenues. *Journal of Cell Biology* **217**, 65-77 (2018).

57 Baar, M. P., Brandt, R. M., Putavet, D. A., Klein, J. D., Derks, K. W. *et al.* Targeted apoptosis of senescent cells restores tissue homeostasis in response to chemotoxicity and aging. *Cell* **169**, 132-147. e116 (2017).

58 Hannan, N. J., Stock, O., Spencer, R., Whitehead, C., David, A. L. *et al.* Circulating mRNAs are differentially expressed in pregnancies with severe placental insufficiency and at high risk of stillbirth. *BMC Medicine* **18**, 145 (2020).